

Erratum to: “Nuclear Effects on $R = \sigma_L/\sigma_T$ in Deep-Inelastic Scattering”
Phys. Lett. B 475 (2000) 386

A. Airapetian,³¹ N. Akopov,³¹ Z. Akopov,³¹ M. Amarian,^{26,31} V.V. Ammosov,²⁴ E.C. Aschenauer,⁶ R. Avakian,³¹
A. Avetissian,³¹ E. Avetissian,³¹ P. Bailey,¹⁵ V. Baturin,²³ C. Baumgarten,²¹ M. Beckmann,⁵ S. Belostotski,²³
S. Bernreuther,²⁹ N. Bianchi,¹⁰ H.P. Blok,^{22,30} H. Böttcher,⁶ A. Borissov,¹⁹ O. Bouhali,²² M. Bouwhuis,¹⁵
J. Brack,⁴ S. Brauksiepe,¹¹ A. Brüll,¹⁸ I. Brunn,⁸ G.P. Capitani,¹⁰ H.C. Chiang,¹⁵ G. Ciullo,⁹ G.R. Court,¹⁶
P.F. Dalpiaz,⁹ R. De Leo,³ L. De Nardo,¹ E. De Sanctis,¹⁰ E. Devitsin,²⁰ P.K.A. de Witt Huberts,²² P. Di Nezza,¹⁰
M. Düren,¹³ M. Ehrenfried,⁶ A. Elalaoui-Moulay,² G. Elbakian,³¹ F. Ellinghaus,⁶ U. Elschenbroich,¹¹ J. Ely,⁴
R. Fabbri,⁹ A. Fantoni,¹⁰ A. Fechtchenko,⁷ L. Felawka,²⁸ H. Fischer,¹¹ B. Fox,⁴ J. Franz,¹¹ S. Frullani,²⁶
Y. Gärber,⁸ G. Gapienko,²⁴ V. Gapienko,²⁴ F. Garibaldi,²⁶ E. Garutti,²² G. Gavrilo, ²³ V. Gharibyan,³¹
G. Graw,²¹ O. Grebeniouk,²³ P.W. Green,^{1,28} L.G. Greeniaus,^{1,28} A. Gute,⁸ W. Haeberli,¹⁷ K. Hafidi,²
M. Hartig,²⁸ D. Hasch,¹⁰ D. Heesbeen,²² F.H. Heinsius,¹¹ M. Heno, ⁸ R. Hertenberger,²¹ W.H.A. Hesselink,^{22,30}
Y. Holler,⁵ B. Hommez,¹² G. Iarygin,⁷ A. Izotov,²³ H.E. Jackson,² A. Jgoun,²³ R. Kaiser,¹⁴ E. Kinney,⁴
A. Kisselev,²³ P. Kitching,¹ K. Königsmann,¹¹ H. Kolster,¹⁸ M. Kopytin,²³ V. Korotkov,⁶ E. Kotik,¹ V. Kozlov,²⁰
B. Krauss,⁸ V.G. Krivokhijine,⁷ L. Lagamba,³ L. Lapikás,²² A. Laziev,^{22,30} P. Lenisa,⁹ P. Liebing,⁶
T. Lindemann,⁵ W. Lorenzon,¹⁹ N.C.R. Makins,¹⁵ H. Marukyan,³¹ F. Masoli,⁹ F. Menden,¹¹ V. Mexner,²²
N. Meyners,⁵ O. Mikloukho,²³ C.A. Miller,^{1,28} V. Muccifora,¹⁰ A. Nagaitsev,⁷ E. Nappi,³ Y. Naryshkin,²³
A. Nass,⁸ K. Negodaeva,⁶ W.-D. Nowak,⁶ K. Oganessyan,^{5,10} H. Ohsuga,²⁹ G. Orlandi,²⁶ S. Podiatchev,⁸
S. Potashov,²⁰ D.H. Potterveld,² M. Raithel,⁸ D. Reggiani,⁹ P.E. Reimer,² A. Reischl,²² A.R. Reolon,¹⁰ K. Rith,⁸
G. Rosner,¹⁴ A. Rostomyan,³¹ D. Ryckbosch,¹² Y. Sakemi,²⁹ I. Sanjiev,^{2,23} F. Sato,²⁹ I. Savin,⁷ C. Scarlett,¹⁹
A. Schäfer,²⁵ C. Schill,¹¹ G. Schnell,⁶ K.P. Schüller,⁵ A. Schwind,⁶ J. Seibert,¹¹ B. Seitz,¹ R. Shandiz,⁸
T.-A. Shibata,²⁹ V. Shutov,⁷ M.C. Simani,^{22,30} K. Sinram,⁵ M. Stancari,⁹ M. Statera,⁹ E. Steffens,⁸
J.J.M. Steijger,²² J. Stewart,⁶ U. Stösslein,⁴ K. Suetsugu,²⁹ H. Tanaka,²⁹ S. Taroian,³¹ A. Terkulov,²⁰
S. Tessarin,⁹ E. Thomas,¹⁰ A. Tkabladze,⁶ M. Tytgat,¹² G.M. Urciuoli,²⁶ G. van der Steenhoven,²²
R. van de Vyver,¹² M.C. Vetterli,^{27,28} V. Vikhrov,²³ M.G. Vincter,¹ J. Visser,²² J. Volmer,⁶ C. Weiskopf,⁸
J. Wendland,^{27,28} J. Wilbert,⁸ T. Wise,¹⁷ S. Yen,²⁸ S. Yoneyama,²⁹ B. Zihlmann,^{22,30} and H. Zohrabian³¹

(The HERMES Collaboration)

¹Department of Physics, University of Alberta, Edmonton, Alberta T6G 2J1, Canada

²Physics Division, Argonne National Laboratory, Argonne, Illinois 60439-4843, USA

³Istituto Nazionale di Fisica Nucleare, Sezione di Bari, 70124 Bari, Italy

⁴Nuclear Physics Laboratory, University of Colorado, Boulder, Colorado 80309-0446, USA

⁵DESY, Deutsches Elektronen-Synchrotron, 22603 Hamburg, Germany

⁶DESY Zeuthen, 15738 Zeuthen, Germany

⁷Joint Institute for Nuclear Research, 141980 Dubna, Russia

⁸Physikalisches Institut, Universität Erlangen-Nürnberg, 91058 Erlangen, Germany

⁹Istituto Nazionale di Fisica Nucleare, Sezione di Ferrara and

Dipartimento di Fisica, Università di Ferrara, 44100 Ferrara, Italy

¹⁰Istituto Nazionale di Fisica Nucleare, Laboratori Nazionali di Frascati, 00044 Frascati, Italy

¹¹Fakultät für Physik, Universität Freiburg, 79104 Freiburg, Germany

¹²Department of Subatomic and Radiation Physics, University of Gent, 9000 Gent, Belgium

¹³Physikalisches Institut, Universität Gießen, 35392 Gießen, Germany

¹⁴Department of Physics and Astronomy, University of Glasgow, Glasgow G12 8QQ, United Kingdom

¹⁵Department of Physics, University of Illinois, Urbana, Illinois 61801, USA

¹⁶Physics Department, University of Liverpool, Liverpool L69 7ZE, United Kingdom

¹⁷Department of Physics, University of Wisconsin-Madison, Madison, Wisconsin 53706, USA

¹⁸Laboratory for Nuclear Science, Massachusetts Institute of Technology, Cambridge, Massachusetts 02139, USA

¹⁹Randall Laboratory of Physics, University of Michigan, Ann Arbor, Michigan 48109-1120, USA

²⁰Lebedev Physical Institute, 117924 Moscow, Russia

²¹Sektion Physik, Universität München, 85748 Garching, Germany

²²Nationaal Instituut voor Kernfysica en Hoge-Energiefysica (NIKHEF), 1009 DB Amsterdam, The Netherlands

²³Petersburg Nuclear Physics Institute, St. Petersburg, Gatchina, 188350 Russia

²⁴Institute for High Energy Physics, Protvino, Moscow oblast, 142284 Russia

²⁵Institut für Theoretische Physik, Universität Regensburg, 93040 Regensburg, Germany

²⁶Istituto Nazionale di Fisica Nucleare, Sezione Roma 1, Gruppo Sanità

and Physics Laboratory, Istituto Superiore di Sanità, 00161 Roma, Italy

²⁷Department of Physics, Simon Fraser University, Burnaby, British Columbia V5A 1S6, Canada

²⁸TRIUMF, Vancouver, British Columbia V6T 2A3, Canada

²⁹Department of Physics, Tokyo Institute of Technology, Tokyo 152, Japan

³⁰Department of Physics and Astronomy, Vrije Universiteit, 1081 HV Amsterdam, The Netherlands

³¹Yerevan Physics Institute, 375036 Yerevan, Armenia

(Dated: May 22, 2003)

This erratum revokes the main conclusion of a Letter that reported measurements of cross sections for deep-inelastic scattering (DIS) of leptons on ^3He and ^{14}N targets, expressed as ratios of σ_A/σ_D to the cross section on a deuterium target. In the particular kinematic domain $x < 0.03$ with $Q^2 < 1.25 \text{ GeV}^2$, σ_A/σ_D was reported to differ as much as 35% from earlier such measurements at higher energies. As the only significant difference from the earlier measurements appeared to be the kinematic variable y , and hence the polarisation parameter ϵ , the new results were interpreted as evidence for a nuclear influence on the ratio R of the cross sections for longitudinal and transverse photons. This anomaly has now been discovered to be due to a peculiar instrumental effect, which was not recognised in the previous analysis. The resulting correction to the cross section ratios is significant at low values of x and Q^2 and substantially changes the interpretation of those data. The data presented here were corrected for this effect and supersede those originally published. For the description of the experiment, the definition of the variables and the constraints imposed on the data, the reader is referred to the original Letter.

To facilitate the interpretation of the data, here and throughout this paper all cross sections are defined as cross sections per nucleon and are converted to cross sections for isoscalar nuclei, i.e. the measured cross sections are divided by the atomic number A and corrected for any difference in the number of protons and neutrons:

$$\frac{\sigma_A}{\sigma_D} \equiv \frac{\sigma_A^{nucleus}}{Z\sigma_p + (A-Z)\sigma_n}, \quad (1)$$

where $\sigma_A^{nucleus}$ is the DIS cross section per nucleus for nucleus A , and σ_p and σ_n are the DIS cross sections on the proton and the neutron. In practice, $\sigma_A^{nucleus}/\sigma_D$ is converted to σ_A/σ_D using the known cross section ratio σ^D/σ^p [1].

As the ratio σ_A/σ_D involves nuclei with different numbers of protons, radiative corrections do not cancel in the ratio. In particular, the yield of radiative processes associated with elastic scattering scales with Z^2 and thus differs for the two target nuclei. At small values of apparent x and Q^2 (inferred from the kinematics of the scattered positron), corresponding to large values of y , the contribution from radiative elastic scattering becomes large. Unlike radiation associated with inelastic processes, which is predominantly emitted in the direction of either the beam lepton (initial state radiation or ISR) or the scattered lepton (final state radiation or FSR), the hard photons associated with nuclear elastic scattering

involve negligible momentum transfer q to the target nucleus (Compton peak). There are two reasons for this. One is that the Bethe-Heitler cross section for radiative elastic processes predicts that in kinematic conditions corresponding to small values of apparent x and Q^2 , the Compton peak becomes much more prominent compared to ISR and FSR, because smaller values of q become kinematically available, and the cross section is modulated by a factor of $1/q^4$. This is illustrated in Fig. 1, which shows the nuclear-elastic Bethe-Heitler cross section in two different coplanar kinematic situations, both with and without including the nuclear form factor. This latter comparison reveals the other reason — that the nuclear form factor strongly suppresses the cross section for significant momentum transfer to the target, leaving only the Compton peak.

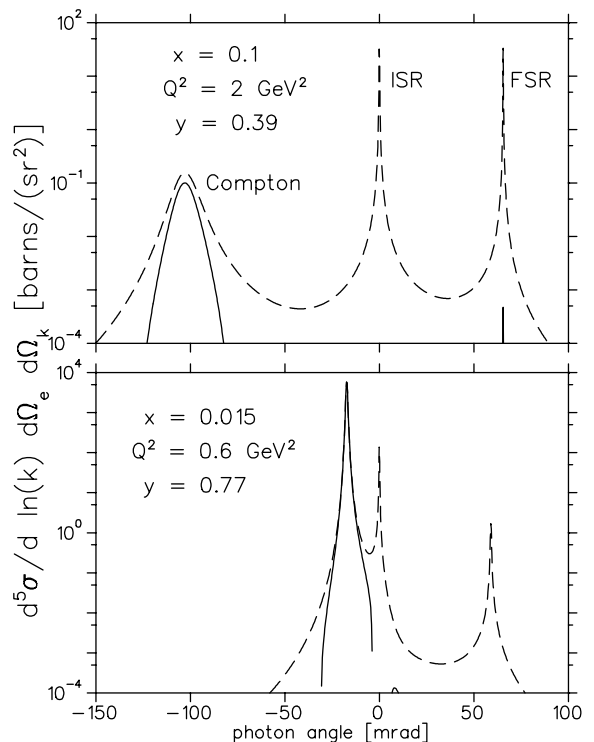


FIG. 1: The nuclear-elastic Bethe-Heitler cross section [2] on ^{14}N for two different coplanar kinematic conditions as labelled in terms of apparent DIS kinematic variables. The continuous curves include the effects of the nuclear form factor.

With negligible nuclear recoil momentum, essentially all of the transverse momentum of the scattered lepton must be balanced by that of the radiated hard photon, which also carries away most of the beam energy at these

large values of apparent y . Hence one has

$$(1 - y) \sin \theta_{e'} = y \sin \theta_\gamma, \quad (2)$$

showing that at large y , the angle of the high-energy photon on the opposite side of the beam line is correspondingly smaller than that of the scattered lepton, but not negligible. In the mirror-symmetric open geometry of the HERMES spectrometer [3], this can have drastic consequences. These energetic photons from nuclear targets have a high probability of hitting the detector frames surrounding the beam line in front of the dipole magnet, and producing extensive electromagnetic showers that cause very high hit multiplicities in these tracking detectors. For many of these nuclear-elastic events, track reconstruction is therefore impossible, resulting in a large tracking inefficiency that is strictly correlated with only this process and kinematic situation.

This problem is pernicious because it is far from apparent in the experimental data. The event trigger rate for real DIS events is typically very small compared to that from hadron background. Only after event reconstruction can all of the particle identification criteria be applied to eliminate the hadrons. However, event reconstruction is impossible for the affected radiative elastic events, so they remain hidden in the dominant hadron background and lost to the analysis, even though they are included in the radiative corrections. A simulation of the experiment reveals the problem only if it includes both the nuclear target with its particular radiative effects, and a complete treatment of showers in material outside of the geometric acceptance. This was not included in the data analysis for the original Letter but has now been simulated using the GEANT-based Monte Carlo description of the experiment. The probability of photon emission is modelled following the description of Mo and Tsai [4], and has been carefully compared to other calculations of radiative processes. The level of agreement was found similar to an earlier comparison for 200 GeV muons [5]. All materials close to the beam pipe have been implemented in detail and the minimum energy of the secondary particles tracked through the detector was chosen to include the effects of the full electromagnetic shower. The resulting reconstruction losses at low x and Q^2 strongly depend on the target material and show a strong variation with y , and consequently with x and Q^2 . The ratios of the reconstruction efficiencies η for target nucleus A compared to deuterium are shown in Fig. 2 as a function of x , for the various target materials used in the HERMES experiment. To demonstrate the kinematic dependence of this correction, this figure includes points at smaller values of x and for one heavier nucleus (Kr) than are employed in the present analysis.

The systematic uncertainty of this correction was estimated using the fact that the HERMES spectrometer consists of two independent detectors above and below the positron beam. For about 50 % of the events

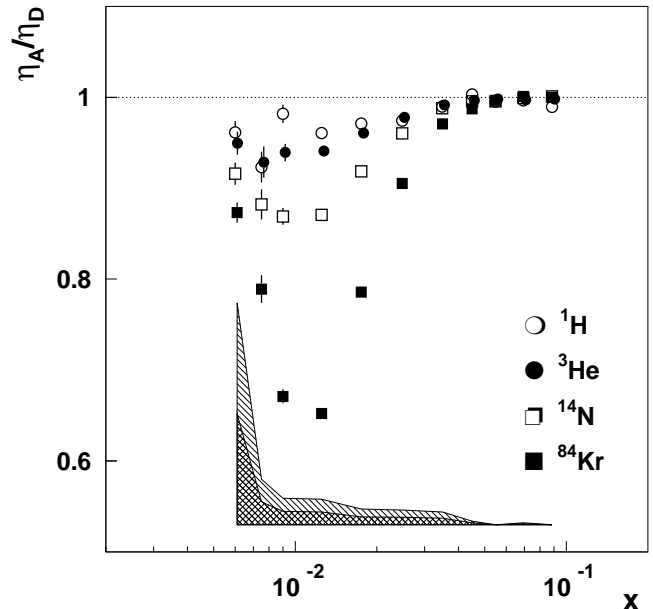


FIG. 2: Ratio of track reconstruction efficiencies in ^1H , ^3He , ^{14}N and ^{84}Kr with respect to ^2H as function of x . The hatched areas represent the systematic uncertainties for the He/D (cross hatched) and N/D (slanted hatched) efficiency ratios relevant for this analysis. The systematic uncertainties for the H/D and Kr/D ratios are not shown.

with a hard radiated photon the resulting electromagnetic shower is contained in one detector while the scattered electron is found in the other detector. While these events are rejected by the standard HERMES reconstruction algorithm because of their high total multiplicity, they can be reconstructed when one considers the two detectors independently. The number of events gained in this way strongly depends on the details of the electromagnetic shower – especially on the energy of the radiated photon and the exact position where the photon hits any material – and thus provides a good measure of the quality of the MC simulation. Reasonable agreement between the data and the simulation is found for all target materials. Fig. 3 shows as a function of apparent x the ratio of fractional changes in the yields of nitrogen and deuterium when treating the upper and lower spectrometer halves independently, both for the data and the MC simulation. The small difference between the yields in the upper and the lower detector observed in the data is attributed to a relative misalignment between the two detectors and is included in the systematic error. The difference between the data and the MC simulation is treated as an additional systematic uncertainty.

The track reconstruction inefficiency mainly affects radiative elastic and to some extent quasielastic events. These and all other radiative processes have been computed using the method outlined in the original Letter. However, in contrast to the original analysis, the effects of

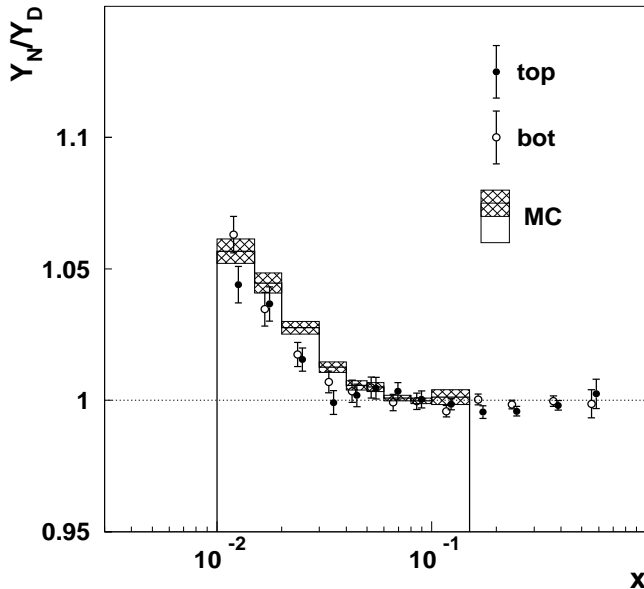


FIG. 3: Comparison between data (open and closed circles) and MC simulation (histogram) for the ratio of fractional changes in the yields of nitrogen and deuterium when treating the upper and lower HERMES detector halves independently.

all radiative processes were subtracted from the measured yields and the statistical errors propagated accordingly. This method avoids the possible large model dependence that can result from multiplicatively applying radiative corrections [6]. Because of the reconstruction inefficiency explained above, only those radiative events actually seen by the HERMES spectrometer were subtracted.

The systematic uncertainty in the radiative corrections was estimated by using upper and lower limits for all the input parameters in the calculations. The resulting systematic uncertainty in the cross section ratio of N/D and He/D is about 4.5 % at low x , quickly falling to values smaller than 1 % for $x > 0.06$. The effects originating from the finite resolution of the spectrometer and from the hadron contamination in the positron sample have been determined and found to be negligible. The overall normalisation uncertainty has been estimated from the luminosity measurements to be 1.4 %.

The results of the present analysis [7] are shown in Fig. 4 as a function of x . Also shown are the results of the NMC [8, 9] and SLAC [10] measurements of σ_{He}/σ_D and σ_C/σ_D . On average, the present data are about 0.9 % below the cross section ratio reported by NMC. A similar difference is observed in comparison to the SLAC data which cover a smaller x but the same Q^2 range than the HERMES data. As the normalisation uncertainty of the present data is considerably larger than that of the NMC data (0.4 %), the HERMES results have been renormalised by 0.9 %. For x values below $x = 0.1$, the present data on N/D are slightly below the NMC data but consistent within the present statistical and system-

atic uncertainties. Such a consistency with NMC of older but previously unpublished data in this kinematic regime was also recently noted for several other nuclei [11].

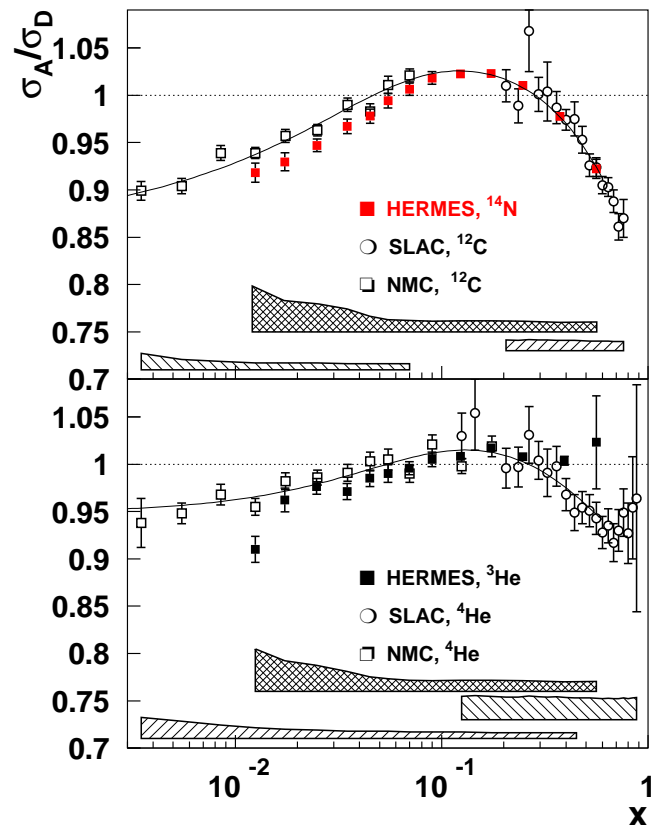


FIG. 4: Ratio of isoscalar Born cross sections of inclusive deep-inelastic lepton scattering from nucleus A and D versus x . The error bars represent the statistical uncertainties, the systematic uncertainties are given by the error bands (ordered as HERMES, SLAC, NMC). The HERMES data have been renormalised by 0.9 %.

The agreement between the different data sets is better illustrated in the upper panel of Fig. 5 where the present σ_N/σ_D data are displayed as a function of Q^2 for fixed values of x together with the NMC data on σ_C/σ_D . No significant Q^2 dependence is observed in the cross section ratio over a wide range in Q^2 .

To investigate a possible A-dependence of $R(x, Q^2)$, the cross section ratios have been fitted as a function of ϵ for fixed values of x . In these fits a parameterisation of R_D [12] has been used, while the ratios R_A/R_D and F_2^A/F_2^D have been treated as free parameters. A single value of R_A/R_D and F_2^A/F_2^D has been extracted from each x -bin. In this procedure it is assumed that both R_A/R_D and F_2^A/F_2^D are constant over the limited Q^2 range covered by the data in each x -bin. The ϵ -dependence of the $^{14}\text{N}/\text{D}$ cross section ratio is shown in the lower panel of Fig. 5. No significant ϵ -dependence is observed. A similar conclusion holds for the $^3\text{He}/\text{D}$ cross section ratio.

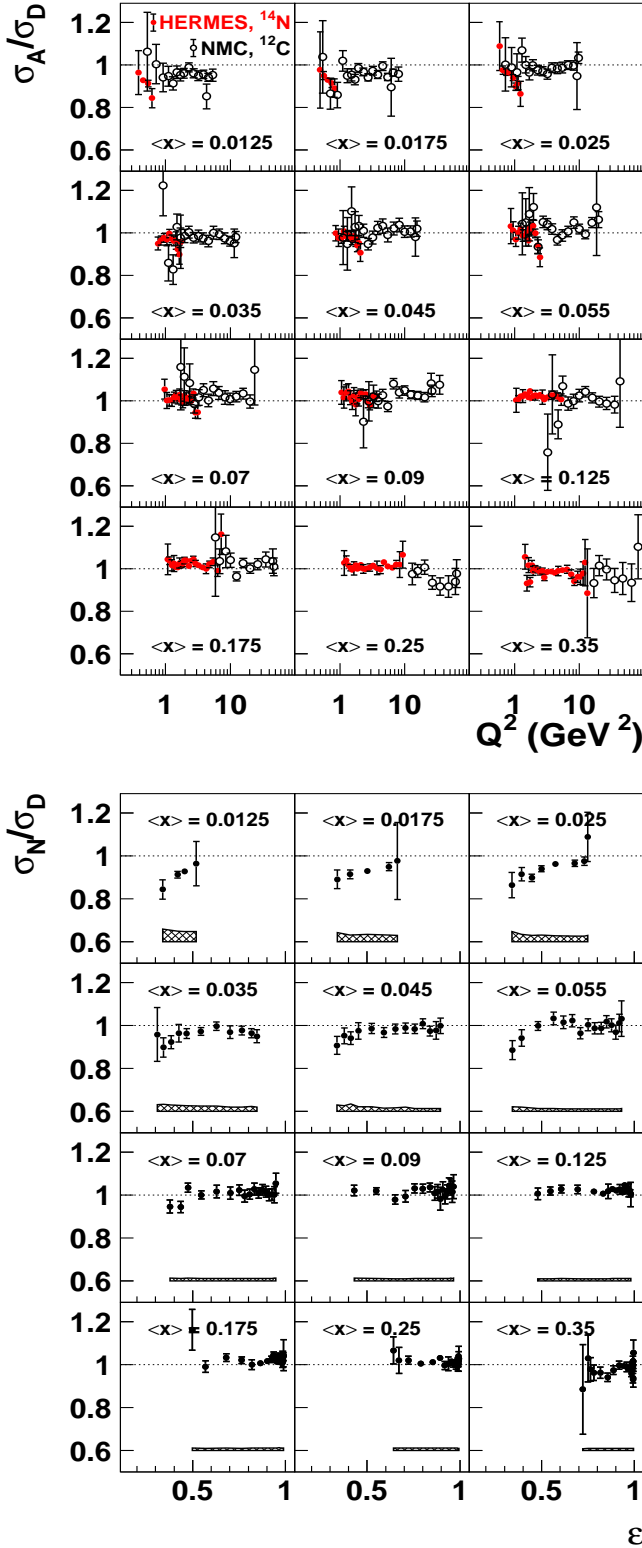


FIG. 5: Ratio of isoscalar Born cross sections of inclusive deep-inelastic lepton scattering from nitrogen and deuterium (renormalised by 0.9 %) for fixed values of x as a function of Q^2 (upper panel) and as a function of ϵ (lower panel). The error bars represent the statistical uncertainties, for the ϵ dependence the systematic uncertainties are given by the error bands.

The values of F_2^A/F_2^D derived from the fit of the HERMES data are found to be consistent with previous measurements of NMC and SLAC. The resulting values of R_A/R_D are shown in Fig. 6. It is worth mentioning that the small systematic errors on R_A/R_D are a result of treating the systematic uncertainties in σ_A/σ_D as fully correlated from point to point. Also shown in this figure are the results of previous studies of the A -dependence of R . Existing data are usually represented in terms of $\Delta R = R_A - R_D$. The published values of ΔR [13–15] have been converted to R_A/R_D using a parameterisation for R_D [12], and added to Fig. 6. The values for the NMC ^{12}C and ^4He data have been derived from the NMC cross section ratios using the same formalism as for the HERMES data. All results for R_A/R_D are found to be consistent with unity.

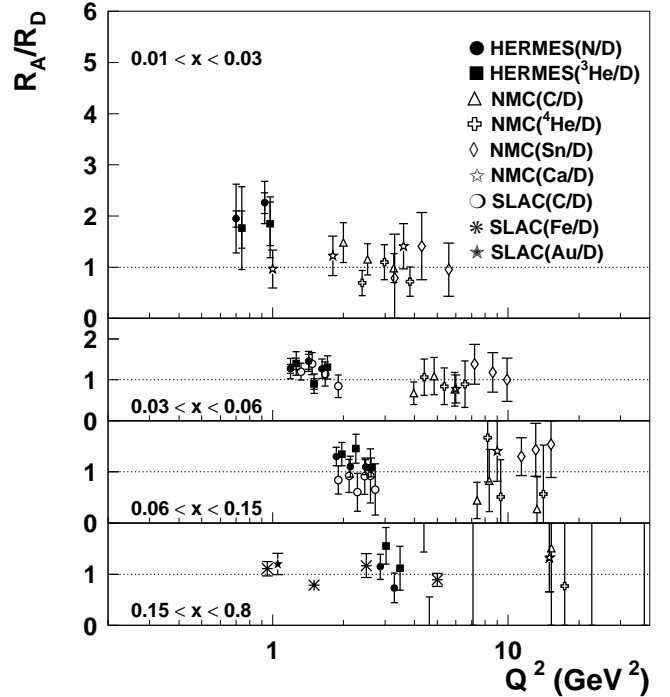


FIG. 6: The isoscalar-corrected ratio R_A/R_D for several nuclei (A) with respect to deuterium as a function of Q^2 for four different x bins. The inner error bars represent the statistical uncertainty and include the correlated error in F_2^A/F_2^D . The outer error bars represent the quadratic sum of the statistical and systematic uncertainties. In the upper panel the HERMES results at the lowest Q^2 value have been suppressed because of its large error bar.

At low x , the HERMES cross section ratios on ^3He and ^{14}N and the NMC measurements on ^4He and ^{12}C have some common Q^2 range. While the NMC measurements at these x and Q^2 values have ϵ values close to unity, the HERMES data cover a typical ϵ range of $0.4 < \epsilon < 0.7$. Combining the two measurements thus increases the precision on R_A/R_D . The results of the fits to the HERMES and NMC data on helium and nitrogen (carbon) are displayed in Fig. 7 as a function of Q^2 together with all other

measurements of R_A/R_D on light and medium heavy nuclei. For Q^2 values between 0.5 and 20 GeV^2 and nuclei from He to Ca, R_A is found to be consistent with the R parametrisation of Whitlow et al [12]. Throughout this analysis, this R parametrisation has been chosen in this comparison because it is dominated by data on the proton and the deuteron. In contrast, the more recent parametrisation by Abe et al. [13] is significantly influenced by nuclear data. The influence of the choice in the R parametrisation is however very small. Averaging over all measurements of R_A/R_D for light and medium heavy nuclei gives an average value for R_A/R_D of 0.99 ± 0.03 .

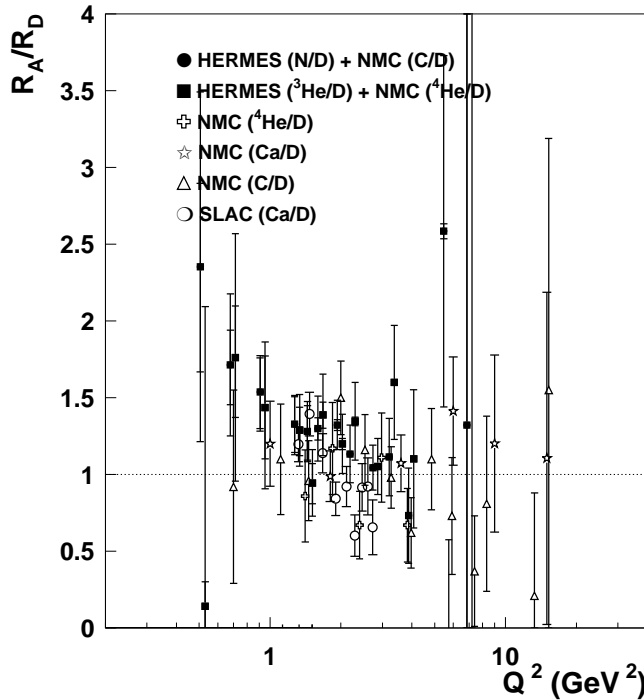


FIG. 7: The isoscalar-corrected ratio R_A/R_D for several nuclei (A) with respect to deuterium as a function of Q^2 . The HERMES and NMC data have been combined in the determination of R_A/R_D . The other data are the same as in Fig. 6.

In summary, revised deep-inelastic positron scattering data on ^2H , ^3He and ^{14}N are presented. After the data were corrected for a previously unrecognised A-dependent tracking inefficiency, the results extracted for the ratios of the DIS cross sections on nuclei to those on the corresponding sets of free nucleons are in agreement with the results from previous measurements. No signif-

icant Q^2 dependence is observed over the wide range in Q^2 covered by the combined data set of HERMES and NMC. Values for the ratio of R_A/R_D with R the ratio σ_L/σ_T of longitudinal to transverse DIS cross sections have been derived from the dependence of the data on the virtual photon polarisation parameter ϵ and found to be consistent with unity.

The kinematic region affected by the correlated background from nuclear targets is restricted to $x < 0.06$ with $Q^2 < 2 \text{GeV}^2$. Polarised DIS data from hydrogen, deuterium and helium-3 targets are unaffected by this background, because of both the more restricted kinematic range, and the much smaller value of Z^2 modulating the elastic Bethe-Heitler cross section. Semi-inclusive data are also unaffected even with nuclear targets [16], as radiative elastic events are excluded by the presence of a hadron in the final state.

-
- [1] M. Arneodo et al. (NMC), Nucl. Phys. B **487** (1997) 3. (2000) 386.
 - [2] C. Itzykson and J.-B. Zuber, *Quantum Field Theory*, New York, McGraw-Hill, 1985 (Eq. 5.150)
 - [3] K. Ackerstaff et al. (HERMES), Nucl. Instr. and Meth. A **417** (1998) 230.
 - [4] Y.S. Tsai, Phys. Rev. **120** (1960) 269; L.W. Mo and Y.S. Tsai, Rev. Mod. Phys. **41** (1969) 205; Y.S. Tsai, SLAC-PUB-848 (1971).
 - [5] D. Bardin, K. Kurek, C. Scholz, B. Badelek, Z. Phys. **C66** (1995) 591.
 - [6] A. Miller, in preparation.
 - [7] E. Garutti, Ph.D. thesis, University of Amsterdam, (2003).
 - [8] P. Amaudruz et al. (NMC), Nucl. Phys. B **441** (1995) 3.
 - [9] M. Arneodo et al. (NMC), Nucl. Phys. B **441** (1995) 12.
 - [10] J. Gomez et al., Phys. Rev. D
 - [11] P. Bosted and S. Rock, hep-ex/0003007.
 - [12] L.W. Whitlow et al., Phys. Lett. B **250** (1990) 193. **49** (1994) 4348.
 - [13] K. Abe et al. (SLAC), Phys. Lett. B **452** (1999) 194.
 - [14] S. Dasu et al. (SLAC), Phys. Rev. D **49** (1994) 5641.
 - [15] P. Amaudruz et al. (NMC), Phys. Lett. B **294** (1992) 120; and M. Arneodo et al. (NMC), Phys. Lett. B **481** (1996) 23. S. Stein et al, Phys. Rev. **D 12** (1975) 1884.
 - [16] K. Ackerstaff et al. (HERMES), Phys. Rev. Lett. **82** (1999) 3025; A. Airapetian et al. (HERMES), Eur. Phys. J. C **20** (2001) 479.